Higgs production in CP-violating supersymmetric cascade decays: probing the 'open hole' at the Large Hadron Collider

Priyotosh Bandyopadhyay
Korea Institute for Advanced Study, Seoul

August 26, 2010
SUSY 10

arXiv:1008.3339 [hep-ph]

Plan

1. CP-volation in MSSM
2. CPX
3. Experimental constraints
4. Cascade production
5. Prospect at the LHC
6. Conclusion

Sources of CP violating phases in MSSM

- In the MSSM, CP-violating phases appear in the μ term of the superpotential,

$$W \supset \mu H_u \cdot H_d$$

- and in the soft-SUSY breaking terms as follows:

$$\begin{aligned}
-\mathcal{L}_{\rm soft} \quad & \supset \\
& \frac{1}{2}(M_3\,\widetilde{g}\widetilde{g} + M_2\,\widetilde{W}\widetilde{W} + M_1\,\widetilde{B}\widetilde{B} + \text{h.c.}) \\
& + \widetilde{Q}^\dagger\,\mathbf{M}^{\mathbf{2}}_{\widetilde{\mathbf{Q}}}\,\widetilde{Q} + \widetilde{L}^\dagger\,\mathbf{M}^{\mathbf{2}}_{\widetilde{\mathbf{L}}}\,\widetilde{L} + \widetilde{u}^*_R\,\mathbf{M}^{\mathbf{2}}_{\widetilde{\mathbf{u}}}\,\widetilde{u}_R + \widetilde{d}^*_R\,\mathbf{M}^{\mathbf{2}}_{\widetilde{\mathbf{d}}}\,\widetilde{d}_R + \widetilde{e}^*_R\,\mathbf{M}^{\mathbf{2}}_{\widetilde{\mathbf{e}}}\,\widetilde{e}_R \\
& - m_1^2 H_d^* H_d - m_2^2 H_u^* H_u - (m_{12}^2 H_u H_d + \text{h.c.}) \\
& + (\widetilde{u}^*_R\,\mathbf{A_u}\,\widetilde{Q}H_u - \widetilde{d}^*_R\,\mathbf{A_d}\,\widetilde{Q}H_d - \widetilde{e}^*_R\,\mathbf{A_e}\,\widetilde{L}H_d + \text{h.c.})
\end{aligned}$$

CP violating phases in MSSM

- Not all are independent.
- Physical ovservables depend on the two combinations:

$$\mathrm{Arg}(M_i\,\mu\,(m_{12}^2)^*)\,, \quad \mathrm{Arg}(A_f\,\mu\,(m_{12}^2)^*)\,,$$

with $i = 1 - 3$ and $f = e, \mu, \tau; u, c, t, d, s, b$.

- Most relevant CP phases pertinent to the Higgs sector:

$$\Phi_i \equiv \mathrm{Arg}(M_i)\,; \quad \Phi_{A_{f_3}} \equiv \mathrm{Arg}(A_{f_3})\,,$$

with $f_3 = \tau, t, b$.

CP violation in MSSM contd.

- CP violation in the Higgs potential of the MSSM leads to mixing terms between the CP-even and CP-odd Higgs fields. ▸ more
  Pilaftsis, etal; 88,98
- In the weak basis (G^0, a, ϕ_1, ϕ_2), the neutral Higgs-boson mass matrix $\mathcal{M}_0^2$ may be cast into the form

$$\mathcal{M}_0^2 = \begin{pmatrix} \widehat{\mathcal{M}}_P^2 & \mathcal{M}_{PS}^2 \\ \mathcal{M}_{SP}^2 & \mathcal{M}_S^2 \end{pmatrix}$$

where,

$$\widehat{\mathcal{M}}_P^2 \Rightarrow \begin{pmatrix} G^0 \\ a \end{pmatrix} \leftrightarrow \begin{pmatrix} G^0 \\ a \end{pmatrix} \qquad \mathcal{M}_S^2 \Rightarrow \begin{pmatrix} \phi_1 \\ \phi_2 \end{pmatrix} \leftrightarrow \begin{pmatrix} \phi_1 \\ \phi_2 \end{pmatrix}$$

$$\mathcal{M}_{PS}^2 = (\mathcal{M}_{SP}^2)^T \qquad \Rightarrow \begin{pmatrix} G^0 \\ a \end{pmatrix} \leftrightarrow \begin{pmatrix} \phi_1 \\ \phi_2 \end{pmatrix}$$

CP violation in MSSM contd.

- G_0 is massless: Doesn't mix with other neutral fields.
- $\mathcal{M}_0^2$ reduces to a (3×3)-dimensional matrix, $\mathcal{M}_N^2$ in the basis (a, ϕ_1, ϕ_2).
- $\mathcal{M}_N^2$ is symmetric, we can diagonalize it by means of an orthogonal rotation O as follows:

$$O^T \mathcal{M}_N^2 O = \mathrm{diag}\,(M_{h_3}^2,\ M_{h_2}^2,\ M_{h_1}^2)\ .$$

- Where,

$$M_{h_1} \leq M_{h_2} \leq M_{h_3}\ .$$

- Do not have any definite CP properties.

The CPX scenario

- The mixing become significant when $\mathrm{Im}(\mu A_t / M^2_{SUSY})$ is large.
- Motivated by this following CP-violating benchmark scenario CPX was introduced in the literature.
  Carena,Pilaftsis, Ellis, Wagner

$$M_{\tilde{Q}_3} = M_{\tilde{U}_3} = M_{\tilde{D}_3} = M_{\tilde{L}_3} = M_{\tilde{E}_3} = M_{\rm SUSY}\,,$$
$$|\mu| = 4\,M_{\rm SUSY}\,, \quad |A_{t,b,\tau}| = 2\,M_{\rm SUSY}\,, \quad |M_3| = 1 \ \ {\rm TeV}.$$

- The parameter $\tan\beta$, $M_{H^\pm}$, and $M_{\rm SUSY}$ can be varied.
- For CP phases, $\Phi_A = \Phi_{A_t} = \Phi_{A_b} = \Phi_{A_\tau}$, we have two physical phases to vary: Φ_A and $\Phi_3 = \mathrm{Arg}(M_3)$.
- Special case:

$$M_{SUSY} = 500 \text{ GeV}, \quad \Phi_A = \Phi_{M_3} = 90^\circ$$
$$M_2 = 2M_1 = 200 \text{ GeV}, \quad \tan\beta = 5 - 10$$

The Experimental constraints

- LEP put a lower bound on SM Higgs: $m_H \geq 114.4$ GeV.
- Similar bound on CPC MSSM Higgs: $m_h \geq 92.9$ GeV.
- The 'LEP hole' in CPX scenario

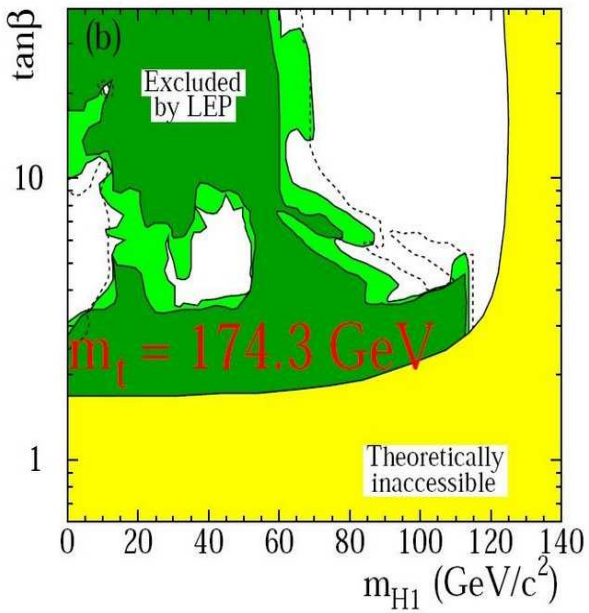

CPX:"LEP-hole" and Earlier works

- $Z - Z - h_1$ coupling goes down.
  $\Rightarrow$ can not probe the CPX.
  $g_{t\bar{t}h_1}$ also goes down.
- Need to find out a channel to probe CPX.
- Sum rule:

$$g^2_{h_i VV} + \mid g_{h_i H^- W^+} \mid^2 = 1$$

$$g^2_{h_i VV} \downarrow \quad \Rightarrow \quad g_{h_i H^- W^+} \uparrow$$

- New channel: $pp \longrightarrow H^+ h_1 \longrightarrow h_1 h_1 W^+ \longrightarrow b\bar{b}b\bar{b}l\nu$
  Moretti, Gosh,
- New channel: $pp \longrightarrow t\bar{t} + X \longrightarrow bbbbqql\nu$
  Gosh, Roy and Godbole
- As $g_{\tilde{t}_1 \tilde{t}_1^* h_1} \uparrow$ and $g_{\tilde{t}_1 \tilde{t}_1^* h_3} \downarrow$
  Low m_{h_1} ($\leq$60 GeV)
  $\Rightarrow \tilde{t}_1 \tilde{t}_1^* h_1 \rightarrow 4b + OSD + \not{p}_T$ can be promising
  Bandyopadhyay, Datta, Datta, Mukhopadhyay

CPX: Mass spectrum

- Mass spectrum (in GeV) in CPX scenario with $\tan\beta$=5 and $m_{H^\pm}$=130 GeV, i.e. BP1.

m_{h_1}	m_{h_2}	m_{h_3}
39.8	104.7	137.1

$m_{\tilde{t}_1}$	$m_{\tilde{t}_2}$	$m_{\tilde{b}_1}$	$m_{\tilde{b}_2}$	$m_{\chi_1^0}$	$m_{\chi_2^0}$	$m_{\chi_1^\pm}$
317.6	668.2	475.9	526.6	99.6	198.4	198.4

Cross-sections

- The cross sections (in fb): computed with `CalcHEP` (interfaced with the program `CPSuperH`)

$\sigma_{\tilde{t}_1\tilde{t}_1^*}$	$\sigma_{\tilde{b}_1\tilde{b}_1^*}$	$\sigma_{\tilde{t}_2\tilde{t}_2^*}$	$\sigma_{\tilde{b}_2\tilde{b}_2^*}$	$\sigma_{\tilde{t}_1\tilde{t}_2}$	$\sigma_{\tilde{b}_1\tilde{b}_2}$	$\sigma_{\tilde{t}_i\tilde{b}_j}$	$\sigma_{\tilde{g}\tilde{g}}$
2861	323.3	4	178.5	8	0.6	7	135

$\tilde{t}_1 \tilde{t}_1^*$ cascade

$\mathrm{Br}(\tilde{t}_1 \to b\chi_1^+)$	$\mathrm{Br}(\tilde{t}_1 \to t\chi_1^0)$
0.81	0.19

- $Br(H^\pm \to h_1 W^\pm) = 0.84 \quad \Rightarrow$ leads to non-trivial signatures
- $\tilde{t}_1 \tilde{t}_1{}^* \to t\bar{t}\chi_1^0\chi_1^0 \to b\bar{b}H^+H^-\chi_1^0\chi_1^0 \to b\bar{b}W^+W^-h_1h_1\chi_1^0\chi_1^0$
- But $\mathrm{Br}(t \to bH^+) \simeq 0.011$
  $\Rightarrow \mathrm{Br}(\tilde{t}_1\tilde{t}_1^* \to b\bar{b}H^+H^-\chi_1^0\chi_1^0) \simeq 5 \times 10^{-6}$

$\tilde{t}_1 \tilde{t}_1^*$ cascade

- If one of the $\tilde{t}_1$ decays via $\tilde{t}_1 \to b\chi_1^+$ and this gives rise to the following signal signal topologies.

$$\tilde{t}_1 \tilde{t}_1{}^* \to t\bar{b}\chi_1^0\chi_1^- \to b\bar{b}H^+W^-\chi_1^0\chi_1^0 \to b\bar{b}h_1W^+W^-\chi_1^0\chi_1^0$$

$$\to 4b + 4(non-b)jet + \not{p}_T$$

$$\to 4b + 1(non-b)jet + 1\ell + \not{p}_T$$

$$\to 4b + OSD + \not{p}_T$$

$\tilde{b}_1 \tilde{b}_1^*$ cascade

$\text{Br}(\tilde{b}_1 \to \tilde{t}_1 H^-)$	$\text{Br}(\tilde{b}_1 \to \tilde{t}_1 W^-)$
0.77	0.12

- $\tilde{b_1} \to \tilde{t_1} H^-$ is very large. $\Rightarrow$ both the $\tilde{b}_1$s can decay in that mode.
- $H^\pm \to h_1 W^\pm$ is also large as this mode is open here.
- Depending on the decay mode of w we can have the following final states.

$$pp \to \tilde{b_1}\tilde{b_1}^* \to \tilde{t_1}\tilde{t_1}^* H^+ H^- \to b\bar{b} W^+ W^- W^+ W^- h_1 h_1 + \not{p}_T$$

$$\to 6b + LSD + 4(non-b)jet + \not{p}_T$$

$$\to 6b + 3\ell + 2(non-b)jet + \not{p}_T$$

$$\to 6b + 4\ell + \not{p}_T$$

Contribution of $\tilde{g}\tilde{g}$cascade

$\mathrm{Br}(\tilde{g} \to b\tilde{b}_1)$	$\mathrm{Br}(\tilde{g} \to b\tilde{b}_2)$	$\mathrm{Br}(\tilde{g} \to t\tilde{t}_1)$	$\mathrm{Br}(\tilde{g} \to t\tilde{t}_2)$
0.28	0.24	0.32	0.16

- $\tilde{g}$ decays to $t\tilde{t}_1$ $b\tilde{b}_1$

  $\Rightarrow \tilde{g}\tilde{g}$ also adds to the cross-section.

Possible parton level signals

Number of channels	Channels	Effective cross-sec (in fb)
1	$6b + LSD + 4(non-b)jet + \not{p}_T$	11.49
1	$6b + OSD + 4(non-b)jet + \not{p}_T$	22.98
2	$6b + 3\ell + 2(non-b)jet + \not{p}_T$	17.24
3	$6b + 4\ell + \not{p}_T$	8.62
4	$4b + 4(non-b)jet + \not{p}_T$	0.38
5	$4b + 1(non-b)jet + 1\ell + \not{p}_T$	0.18
6	$4b + OSD + \not{p}_T$	0.09

Table: Production cross sections (in fb) at lowest-order computed with `CalcHEP` interfaced with CPsuperH for different signal processes at the LHC in the CPX scenario and for the spectrum of BP1.

Set up for the numerical session

- Event generation: `CalcHEP` interfaced with`CPSuperH`.
- (Generated events + Relevant CPV-Brs) $\Rightarrow$ passed to PYTHIA(via SLHA).
- ISR/FSR, hadronization and jet formation: from PYTHIA.

Kinematical distributions

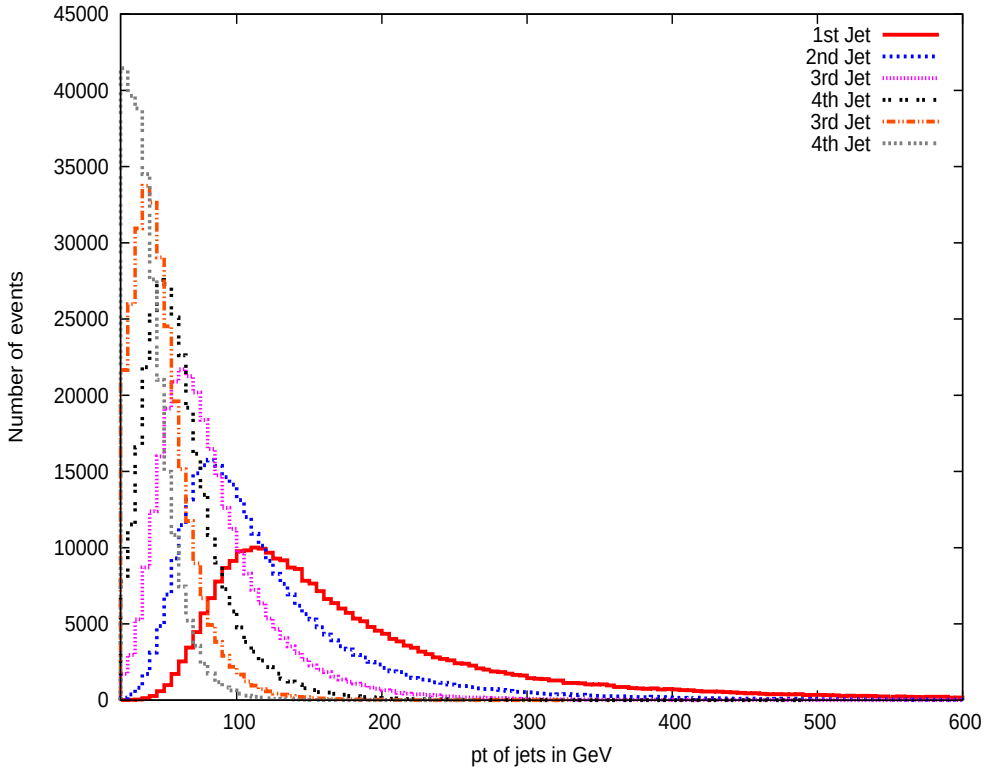

Figure: Ordered p_T^{jet} distributions in CPV-SUSY scenario for $\tilde{b}_1 \tilde{b}_1^*$

Backgrounds

- The main background for this case is $t\bar{t}$
- The other main SM backgrounds are $t\bar{t}Z$ and $t\bar{t}b\bar{b}$

Kinematical distributions

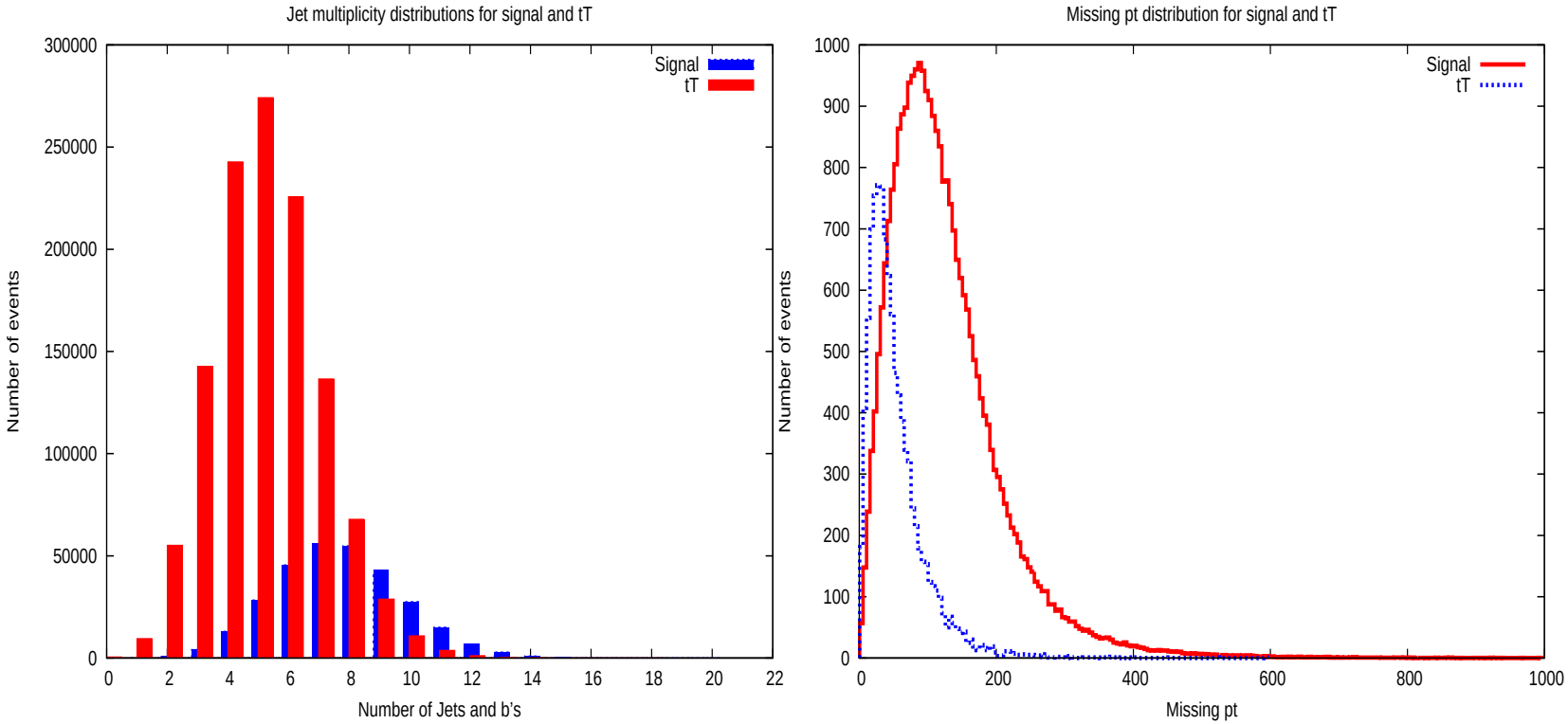

Figure: Ordered p_T^{jet} (left) and parton level b p_T distributions in CPV-SUSY scenario for $\tilde{b}_1 \tilde{b}_1^*$

Results for signals

No.	Signal topology	$\tilde{b}_1\tilde{b}_1^*$	$\tilde{t}_1\tilde{t}_1^*$	$\tilde{g}\tilde{g}$
1	$n_{jet} \geq 8(b-\text{jet} \geq 3) + l \geq 2 + \not{p}_T \geq 100$	10(5.6)	0.4(0.2)	53(52.8)
2	$n_{jet} \geq 8(b-\text{jet} \geq 3) + l \geq 2(\text{OSD} \geq 1) + \not{p}_T \geq 100$	7(3.9)	0.4(0.2)	37(36.7)
3	$n_{jet} \geq 8(b-\text{jet} \geq 3) + l \geq 2(\text{SSD} \geq 1) + \not{p}_T \geq 100$	4(2.2)	0(0)	23(22.1)
4	$n_{jet} \geq 8(b-\text{jet} \geq 2) + l \geq 3 + \not{p}_T \geq 100$	2(1.1)	0(0)	8(8)
5	$n_{jet} \geq 8(b-\text{jet} \geq 2) + l \geq 4 + \not{p}_T \geq 100$	0(0)	0(0)	1(0.8)
6	$n_{jet} \geq 8(b-\text{jet} \geq 4) + l \geq 1 + \not{p}_T \geq 100$	3(1.5)	0(0)	34(33.2)
7	$n_{jet} \geq 4(b-\text{jet} \geq 3) + l \geq 1 + \not{p}_T \geq 100$	116(63.6)	45(26.2)	283(279.3)
8	$n_{jet} \geq 4(b-\text{jet} \geq 3) + l \geq 2(\text{OSD} \geq 1) + \not{p}_T \geq 100$	21(9.7)	4(1.9)	54(52.9)
9	$n_{jet} \geq 8(b-\text{jet} \geq 3) + \not{p}_T \geq 100$	149(96.3)	46(34.2)	499(498)

Table: Event rates for the CPX point(BP1) of an integrated luminosity of 10 fb^{-1}

- $p_T \geq 20$ GeV isolated leptons were demanded.

Results for background

No.	Signal topology	$t\bar{t}$	$t\bar{t}Z$	$t\bar{t}b\bar{b}$
1	$n_{jet} \geq 8(b-\text{jet} \geq 3) + l \geq 2 + \not{p}_T \geq 100$	19(13)	0.33(0.27)	6.1(4.6)
2	$n_{jet} \geq 8(b-\text{jet} \geq 3) + l \geq 2(\text{OSD} \geq 1) + \not{\text{p}}_\text{T} \geq 100$	17(12)	0.29(.23)	6.1(4.6)
3	$n_{jet} \geq 8(b-\text{jet} \geq 3) + l \geq 2(\text{SSD} \geq 1) + \not{\text{p}}_\text{T} \geq 100$	3(1)	0.05(0.05)	0(0)
4	$n_{jet} \geq 8(b-\text{jet} \geq 2) + l \geq 3 + \not{p}_T \geq 100$	0(0)	0.27(0.19)	0(0)
5	$n_{jet} \geq 8(b-\text{jet} \geq 2) + l \geq 4 + \not{p}_T \geq 100$	0(0)	0.0(0.0)	0(0)
6	$n_{jet} \geq 8(b-\text{jet} \geq 4) + l \geq 1 + \not{p}_T \geq 100$	5(5)	0.08(0.05)	2.6(2.4)
7	$n_{jet} \geq 4(b-\text{jet} \geq 3) + l \geq 1 + \not{p}_T \geq 100$	1890(953)	22.6(13.21)	297.1 (170.4)
8	$n_{jet} \geq 4(b-\text{jet} \geq 3) + l \geq 2(\text{OSD} \geq 1) + \not{\text{p}}_\text{T} \geq 100$	226(101)	2.7(1.4)	34.2(16.6)
9	$n_{jet} \geq 8(b-\text{jet} \geq 3) + \not{p}_T \geq 100$	1109(784)	13.4(10.5)	252.3(185.6)

Table: Event rates for the CPX point(BP1) of an integrated luminosity of 10 fb^{-1}

Results and signifiance

- $\tilde{t}_1 \tilde{t}_1^*$ contributes mostly for the low jet multiplicity signals
- For the higher jet multiplicity the maximum contribution comes from $\tilde{g}\tilde{g}$
- Comparing the signal and backgrounds, we can get a significance $\geq 10\sigma$ for almost all the signal topologies.
- Except for signal topology 7; where it is of 4.81σ.
- Now two $b-jets$ from the $\tilde{t}_1$ are of high p_T which are not there in SM backgrounds
- We demand $p_T^{j_1,J_2} \geq 100$ GeV.
- Implementation of these cuts increases the signal significance by 10-20%. ▸ more

Other parameter points

- We extend this analysis to the other points of the 'LEP-hole'

Parameters	BP2	BP3	BP4
$\tan\beta$	4.0	4.0	7.0
$m_{H^\pm}$	140	135	125
m_{h_1} (GeV)	49.45	33.8	40.8

Table: Benchmark points within the LEP-hole in m_{h_1}-$\tan\beta$ plane.

- 5σ significance can be achieve with an integrated luminosity of 5-10 fb^{-1}.

Conclusion

- CP-violating SUSY cascade decay can probe the 'LEP-hole' in the CPX scenario with the early data from LHC.
- These types of final states in the CPX scenario are a consequence of low mass of the lightest Higgs boson (as light as 30 GeV)
- Invariant mass distribution of these b-jets can reconstruct the mass of lightest neutral Higgs boson.
- Moreover multi-lepton final states are easy to detect as they are almost background free.
- Finally the supersymmetric cascades under CP-violating scenario are very different from the CP-conserving case because of the possible non-trivial decay modes in the former case.

THANK YOU

CP violation in MSSM

- The Lagrangian describing the MSSM Higgs potential:

$$\begin{aligned}\mathcal{L}_V &= \mu_1^2(\Phi_1^\dagger\Phi_1) + \mu_2^2(\Phi_2^\dagger\Phi_2) + m_{12}^2(\Phi_1^\dagger\Phi_2) + m_{12}^{*2}(\Phi_2^\dagger\Phi_1) \\ &+ \lambda_1(\Phi_1^\dagger\Phi_1)^2 + \lambda_2(\Phi_2^\dagger\Phi_2)^2 + \lambda_3(\Phi_1^\dagger\Phi_1)(\Phi_2^\dagger\Phi_2) \\ &+ \lambda_4(\Phi_1^\dagger\Phi_2)(\Phi_2^\dagger\Phi_1)\end{aligned}$$

- The Higgs superfields are given by $H_u{=}\Phi_2$ and $H_d{=}\tilde{\Phi}_1 = i\tau_2\Phi_1^*$($\tau_2$ is the usual Pauli matrix)

CP violation in MSSM contd.

- $$\Phi_1 = \begin{pmatrix} \phi_1^+ \\ \frac{1}{\sqrt{2}}(v_1 + \phi_1 + ia_1) \end{pmatrix}, \Phi_2 = e^{i\xi} \begin{pmatrix} \phi_2^+ \\ \frac{1}{\sqrt{2}}(v_2 + \phi_2 + ia_2) \end{pmatrix}$$

  $v_1, v_2 \longrightarrow$ VEVs. of the Higgs doublets.
  $\xi \longrightarrow$ is their relative phase.

CP violation in MSSM contd.

- At the tree level, the parameters are given by

$$\mu_1^2 = -m_1^2 - |\mu|^2 \qquad \mu_2^2 = -m_2^2 - |\mu|^2 \qquad \lambda_1 = \lambda_2 = \frac{1}{8}(g_w^2 + g'^2)$$

$$\lambda_3 = -\frac{1}{4}(g_w^2 - g'^2), \qquad \lambda_4 = \frac{1}{2}g_w^2,$$

- Where, g_w, g' are the $SU(2)_L$, $U(1)_Y$ gauge couplings respectively and m_1^2, m_2^2 and m_{12}^2 are soft-SUSY-breaking parameters.

CP violation in MSSM contd.

- These can be fixed by requiring the vanishing of the following tadpole parameters:

$$
\begin{aligned}
T_{\phi_1} &\equiv \langle \frac{\partial \mathcal{L}_V}{\partial \phi_1} \rangle = v_1 \left[\mu_1^2 + \Re e(m_{12}^2 e^{i\xi}) \tan\beta - \frac{1}{2} M_Z^2 \cos 2\beta \right] \\
T_{\phi_2} &\equiv \langle \frac{\partial \mathcal{L}_V}{\partial \phi_2} \rangle = v_2 \left[\mu_2^2 + \Re e(m_{12}^2 e^{i\xi}) \cot\beta + \frac{1}{2} M_Z^2 \cos 2\beta \right] \\
T_{a_1} &\equiv \langle \frac{\partial \mathcal{L}_V}{\partial a_1} \rangle = v_2 \Im m(m_{12}^2 e^{i\xi}) \\
T_{a_2} &\equiv \langle \frac{\partial \mathcal{L}_V}{\partial a_2} \rangle = -v_1 \Im m(m_{12}^2 e^{i\xi})
\end{aligned}
$$

CP violation in MSSM contd.

- where
  $\tan\beta = v_2/v_1 \quad M_Z^2 = (g_w^2 + g'^2)v^2/4 \quad v^2 = v_1^2 + v_2^2.$
- The orthogonal rotation of the CP-odd fields,

$$\begin{pmatrix} a_1 \\ a_2 \end{pmatrix} = \begin{pmatrix} \cos\beta & -\sin\beta \\ \sin\beta & \cos\beta \end{pmatrix} \begin{pmatrix} G^0 \\ a \end{pmatrix}, \qquad (2)$$

  gives rise to a flat direction in the Higgs potential with respect to the G^0 field, i.e. $\langle \partial \mathcal{L}_V / \partial G^0 \rangle = 0$.
- Newly defined basis: mass matrix of the CP-odd scalars becomes diag$(0,\ M_a^2)$
  $\Rightarrow G^0$ field becomes the Goldstone boson, which is absorbed by the longitudinal component of the Z boson.

CP violation in MSSM contd.

- But, the orthogonal rotation leads to a non-trivial CP-odd tadpole parameter given by

$$T_a \equiv \langle \frac{\partial \mathcal{L}_V}{\partial a} \rangle = -v\, \Im m(m_{12}^2 e^{i\xi})$$

- At the tree level, we choose ξ such that $m_{12}^2 e^{i\xi}$ is a real number $\Rightarrow T_a = 0$.

$\Rightarrow$ CP-Conserved.

- Beyond tree level, $m_{12}^2 e^{i\xi}$ acquires a imaginary part.

$\Rightarrow$ CP-violation.

CP violation in MSSM contd.

- The mixing term :

$$\mathcal{M}^2_{SP} = -\frac{T_a}{v}\begin{pmatrix} s_\beta & c_\beta \\ -c_\beta & s_\beta \end{pmatrix} \simeq \mathcal{O}\left(\frac{m_t^4}{v^2}\frac{|\mu||A_t|}{32\pi^2 M^2_{\rm SUSY}}\right)\sin\phi_{\rm CP}$$

  where,
  $\phi_{\rm CP} = \arg(A_t\mu) + \xi \quad M^2_{\rm SUSY} = \frac{1}{2}\left(m^2_{\tilde{t}_1} + m^2_{\tilde{t}_2}\right)$

- CP-phases of gnuino mass parameter also contribute through the threshold corrections $\sim f(M^*\mu^*)$. back

Distinguishing from CPC case

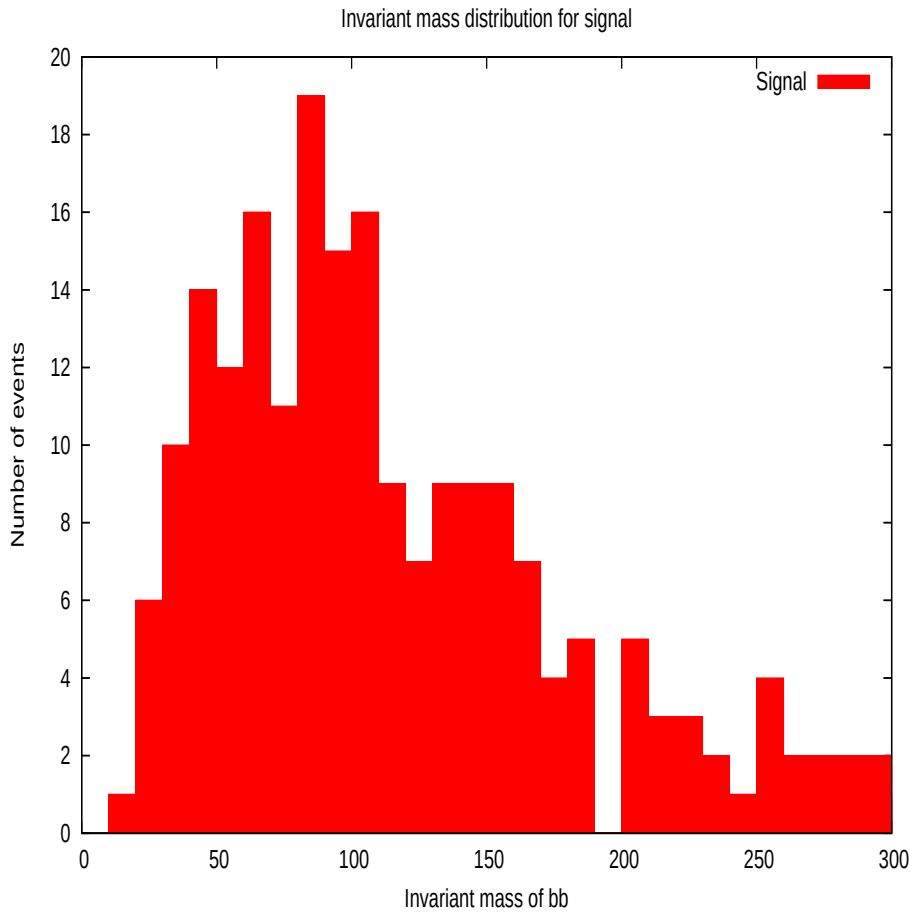

Figure: Invariant mass distribution for $\tilde{b}_1 \tilde{b}_1^*$ in GeV.